

SOME ADVANCES IN EXPERIMENTATION SUPPORTING DEVELOPMENT OF
VISCOPLASTIC CONSTITUTIVE MODELS*

J.R. Ellis and D.N. Robinson†
University of Akron
Akron, Ohio 44325

The primary aim of this paper is to describe the design and development of a biaxial extensometer capable of measuring axial, torsion, and diametral strains to near-microstrain resolution at elevated temperatures. An instrument with this capability was needed to provide experimental support to the development of viscoplastic constitutive models. The operation of the instrument is described first in general terms. Attention is then concentrated on the method of torsional strain measurement. This emphasis is in keeping with the second aim of the paper which is to highlight the advantages gained when torsional loading is used to investigate inelastic material response at elevated temperatures.

The development of the biaxial extensometer was conducted in two stages. The first involved a series of bench calibration experiments performed at room temperature. These experiments investigated characteristics such as linearity and crosstalk over the maximum measurement ranges practicable with the instrument. The second stage of development involved a series of in-place calibration experiments conducted at room and elevated temperatures. The aim of these experiments was to investigate features such as signal stability and signal noise levels under actual test conditions. A review of the torsional calibration data indicated that all performance requirements regarding resolution, range, stability and crosstalk had been met by the subject instrument over the temperature range of interest, 20 to 650 °C.

On completing the instrument development work, the scope of the in-place calibration experiments was expanded to investigate the feasibility of generating stress relaxation data under torsional loading. This approach was found to be practicable and a number of exploratory tests were conducted. The data generated in these experiments were found to be in reasonable agreement with predictions made using the Robinson viscoplastic constitutive model. Also, the experimental data were used successfully to quantify the kinematic state variable in this model. The results of this study showed that the stress relaxation test conducted under torsional loading can be used to advantage in supporting the development of viscoplastic constitutive models.

*Research sponsored by the Office of Breeder Technology Projects, U.S. Department of Energy under Contract W-7405-ENG-26 with the Union Carbide Corporation and by NASA Lewis Research Center under Grant NAG 3-379.

†Resident Research Associates, NASA Lewis Research Center.

INTRODUCTION

One activity within the High Temperature Structural Design Program at the Oak Ridge National Laboratory (ORNL) is the development of constitutive equations for structural alloys intended for Advanced Reactor Systems. These equations were first developed using concepts borrowed from classical plasticity and classical creep (Ref. 1). Experiments conducted in support of this work included investigations of yield and hardening behavior under biaxial loading (Refs. 2 through 5). The type of loading used for this work was tension-torsion and the type of specimen was the thin-walled tube. It was possible, at temperatures in the range 20°C to 232°C, to use foil strain gage rosettes to measure the axial and torsional components of strain. The near-microstrain resolution of these gages allowed small-offset (10 $\mu\epsilon$) yield behavior to be investigated without causing significant changes to the material's state.

More recently, a viscoplastic constitutive model was developed at ORNL which makes use of two internal state variables (Refs. 6 and 7). It was planned to conduct biaxial experiments at temperatures in the range 20°C to 538°C to verify the multiaxial form of this model and also to quantify the internal state variables. The lack of suitable high-temperature strain gages meant that the strain measurement technique used in the earlier experiments could not be used for this work. Since the specimen geometry and the type of loading were relatively simple, it appeared that this would be a suitable application for a biaxial extensometer. However, a detailed review of the literature revealed that existing instruments were not suited to high-precision, probing type experiments at elevated temperatures. This led to an effort being started at ORNL to design and develop such an instrument.

The design requirements for the instrument were based in part on the performance of foil strain gages at room temperature. It was required that the extensometer have near-microstrain resolution while allowing measurement of axial strains and shear strains (engineering) as high as $\pm 20,000 \mu\epsilon$. An additional requirement was that the instrument should be capable of measuring diametral strains up to $\pm 10,000 \mu\epsilon$. This was because it was planned to add internal pressure to the types of loading available for these experiments. It was required that this performance should be maintained up to 650° C.

The type of diametral extensometer developed by Slot et al for high temperature, low cycle fatigue testing was used as a starting point for the subject instrument. Two such diametral extensometers, termed sensors in the following, were used in conjunction with a system of levers to make the biaxial measurements. As might be expected, a lengthy period of development was needed to achieve the required level of performance.

The approach adopted was to first evaluate the instrument on the bench using a biaxial calibration fixture. Such experiments allowed the instrument's characteristics to be investigated at room temperature under closely controlled conditions. A series of in-place calibration experiments was then conducted with the extensometer positioned on strain gaged specimens. Initially, these experiments were conducted at room temperature so that direct comparisons could be drawn between the two strain measurement systems. Subsequently, the emphasis was shifted to investigating

performance at elevated temperatures. Characteristics of interest here were linearity, resolution, crosstalk, mechanical hysteresis, signal noise levels and signal stability.

Finally, exploratory tests were conducted to evaluate the instrument's performance in controlling experiments at elevated temperatures. One such series of tests was aimed at establishing whether the extensometer had sufficient resolution and stability to allow stress relaxation behavior to be investigated under purely torsional loading. This was of particular interest since interpretation of earlier stress relaxation data for 2-1/4 Cr-1 Mo steel, determined under uniaxial loading, had been complicated by coupling between specimen heating and specimen loading. It was anticipated that such coupling, discussed in detail later in the paper, would not be a factor in tests involving torsional loading.

This paper is written in three parts. The first describes the design and development of the ORNL biaxial extensometer, with particular emphasis being given to the method of torsional strain measurement. The second part describes a series of stress relaxation tests performed on 2-1/4 Cr-1 Mo steel under cyclic torsional loading. Finally, comparisons are drawn between the results of these experiments and theoretical predictions made using the Robinson viscoplastic model.

DESIGN AND DEVELOPMENT OF A HIGH-PRECISION BIAxIAL EXTENSOMETER

In designing high temperature extensometers, a number of advantages result if the body of the device is maintained at or near room temperature during elevated temperature tests. This situation can be achieved by using localized specimen heating, ceramic sensing probes, heat shields, and some form of cooling. Adopting these measures, room temperature transducers can be located on the body of the instrument and used in effect for high temperature strain measurement.

Another desirable feature of extensometers is that mechanisms can be incorporated to magnify specimen displacements before they are sensed by the transducers. Such magnification can be an important factor in achieving good resolution in tests involving small strains. One design which successfully incorporates these features in a relatively straightforward manner is the diametral extensometer developed for high temperature, low cycle fatigue testing (Ref. 8). With this simplicity and the need for diametral strain measurements in mind, it was decided to use this instrument as a starting point for the subject biaxial extensometer.

BASIC APPROACH

The basic approach is illustrated schematically in Fig.(1). Two sensors of the type shown in Fig (1a) are positioned on the specimen. These sensors incorporate ceramic probes which grip the specimen by means of friction. The assumption is that once installed, the point of contact of each probe remains fixed on the specimen. The probes serve, therefore, to transmit specimen displacements and rotations to the body of the instrument. A further assumption is that a suspension system

can be designed which constrains the sensors to planes parallel to the X-Y plane of Fig (1b). Two such planes are the DEFG and the HIJK planes shown in this figure.

The method of strain measurement is as follows. Under axial loading, the vertical distance between the sensors, BB in Fig (1b), changes and is used as a basis for axial strain measurement. This is achieved by positioning proximity transducers on the top sensor and a target on the bottom sensor. Regarding diametral strain measurement, loading in the radial sense resulting from internal pressure causes the specimen diameter to change. These changes are transmitted via the hinge to the mounting arms. Relative movement between the mounting arms, AA in Fig (1a), is used for diametral strain measurement. This is accomplished by positioning the core of a linear variable differential transformer (LVDT) on one mounting arm and the coil on the other. Under torsional loading, the sensors rotate different amounts about the Z axis within their respective reference planes. This difference in angular rotation, θ in Fig (1b), is used for torsional strain measurement. The various mechanisms and transducers used in making torsional measurements will be discussed in detail later in the paper.

Regarding the mechanical details, the instrument consists of three subassemblies; the sensors; the lever-arms; and the support structure. One of the extensometers two sensors is shown in Fig (2). The more important components of this subassembly are the ceramic probes, the elastic hinge, the mounting arms, and the preload spring. The function of the spring is to force the probes against the specimen to provide the frictional force necessary to prevent slippage. The strain gages mounted on the probes are monitored during this process to control the amount of preloading. The transducer mounting block is used to grip the coil of the LVDT used for diametral strain measurement. The core of this transducer is shown positioned on the null adjustment screw. Also shown in Fig (2) are the heat shields and water cooling arrangement used to prevent heat buildup in the instrument. Elimination of this effect was viewed as being desirable in isothermal tests and essential in the case of non-isothermal tests.

One of the instrument's four lever-arm assemblies is shown in Fig. (3). The primary function of these assemblies is, in conjunction with the sensors, to transmit specimen rotation to four rotary variable differential transformers (RVDTs) positioned on the support structure. These mechanisms can be thought of as consisting of two levers, BC and CD, which are free to rotate about the vertical axes designated B, C, and D. Such rotation is allowed by flexural pivots which act as bearings (Ref. 9). One end of the lever-arm is bolted to the sensor and the other to the support structure. This arrangement allows the sensors freedom to rotate and displace within planes perpendicular to the three axes. The larger of the two levers, BC, includes a parallel linkage which allows the sensors to displace vertically. At the same time, the parallel linkages ensure that the sensors are constrained to planes which are parallel to the original reference plane. Use is again made of flexural pivots in these linkages as they allow rotation with no associated friction.

The primary function of the instrument's support structure, Fig(4) is to provide a means of mounting the device on the test system or on a calibration fixture. This subassembly consists of a cross-arm which when suitably supported, facilitates positioning of the instrument prior

to testing or calibration. Two vertical posts are attached to the cross-arm and provide mounting locations for the lever-arm assemblies and the RVDTs. One further function of the support structure is to provide a means of supporting the sensors at their centers of gravity on soft vertical springs. This is accomplished using two support brackets which bolt directly to the cross-arm. In addition to housing the spring holders, the support brackets provide convenient mounting locations for the instrument's electrical connectors. This approach has the advantage of isolating the instrument from long lengths of cable.

The complete instrument is shown positioned on a calibration fixture in Fig (5). This figure serves to show the complexity of the assembled instrument. The method of suspending the sensors on springs is shown in this figure along with the method of mounting the electrical connectors.

DETAILS OF TORSIONAL STRAIN MEASUREMENT

The method of torsional strain measurement is shown in more detail in Figs (6) and (7). In the first of these figures, the sensors are considered to be two levers, AB and AE, which have a fixed angle between them and which are constrained to follow the rotation of the specimen. The lever-arms are idealized into three bearing/two lever systems which are supported at points D and G. This mechanism was analyzed to determine the relationship between specimen rotation, θ , and the corresponding lever-arm rotations at the support points, α and α' . The results of this analysis are shown in Fig (7). Here, it can be seen that the relationships between specimen rotation and individual lever-arm rotation are highly nonlinear. However, the curve relating specimen rotation, θ , with the sum of the rotations at the support points, $\alpha + \alpha'$, can be seen to be near-linear. Thus, by positioning RVDTs at the support points, D and G, and summing their outputs electronically, near-linear relationships are obtained between specimen rotation and summed transducer output. By summing in turn the outputs from the two sensors, a combined output is obtained which is proportional to torsional strain as defined in Fig (7).

One problem peculiar to biaxial and multiaxial extensometers is that interaction or crosstalk can occur between the various forms of straining. The mechanism by which specimen displacements in the axial sense can affect torsional strain measurements is shown in Fig. (8). Such displacements cause the parallel linkages incorporated in arms BC and EF to assume some angular position, δ , relative to the original reference plane. These rotations cause the projected lengths of arms BC and EF to shorten in this plane. This shortening in turn causes lever CD to rotate $-\alpha$ from its original position and lever FG to rotate $+\alpha$ from its original position. These rotations are sensed by the RVDTs positioned at locations D and G. However, since the outputs from these RVDTs are summed before being used for measurement purposes, it might be expected that the effect would be self-cancelling. In practice, this situation would only be realised if the lever-arms were manufactured and assembled so as to be identical. With this in mind, the four lever-arms were assembled with extreme care using a special purpose jig. Also, the support structure was designed to provide the linear and angular adjustments necessary during final assembly to achieve the self-cancelling condition.

EVALUATION OF THE BIAxIAL EXTENSOMETER'S PERFORMANCE IN MEASURING TORSIONAL STRAIN

The instrument's performance in measuring torsional strain was evaluated in two stages. The first involved a series of bench calibration experiments conducted at room temperature. A biaxial calibration fixture was designed and developed at ORNL specifically for this work. The aim of these experiments was to investigate linearity and crosstalk over the maximum measurement ranges practicable with instrument.

The second stage of the evaluation involved a series of in-place calibration experiments conducted on thin-walled tubular specimens instrumented with foil strain gage rosettes. The aim here was to investigate mechanical hysteresis, linearity and crosstalk over small strain ranges, say $\pm 100\mu\epsilon$. This was accomplished by loading the specimen within its elastic range and drawing direct comparisons between strain measurements made using the extensometer with those made using the strain gages. This was the preferred evaluation technique in the case of small strains as it avoided placing unrealistic demands on the performance of the calibration fixture.

BENCH CALIBRATION EXPERIMENTS

The fixture used for the bench calibration experiments is shown in Fig.(9). The more important components of this fixture are the micrometer heads used for diametral and axial calibrations and the rotary table used for torsional calibrations. The fixturing shown attached to the diametral micrometer head is designed for diametral calibration work. That shown positioned on the rotary table in Fig. (5) allows axial and torsional calibration. In addition to routine calibration work, the fixture was used to establish ranges of linearity and also to investigate crosstalk between the various types of straining.

The approach adopted in determining torsional calibration data is shown in Fig (5). The extensometer's probes were positioned on the simulated specimen which in turn was positioned on the rotary table of the calibration fixture. The voltage outputs from the RVDTs associated with the top and bottom sensors were monitored after being summed in filter/amplifier modules. The procedure followed in these experiments was to rotate the simulated specimen through known angles and to note the corresponding RVDT output. The angular calibration data generated in this manner for the range ± 60 arc-min. are shown in Fig (10). As indicated on this figure, the extensometer was removed from the calibration fixture and then reinstalled at total of six times in generating the data shown. This procedure was followed to determine the repeatability of the calibration data.

The multiaxial calibration fixture was also used to investigate crosstalk between axial and torsional straining. The approach adopted here was to set known angular rotations and then to note the change in RVDT output as axial displacements in the range ± 1.27 mm were superimposed using the calibration fixture's axial micrometer head. This range of displacements corresponds to an axial strain range of $\pm 50,000 \mu\epsilon$, assuming a 25.4 mm specimen gage length. Data generated for angular settings in the range 0 to +60 arc-min. are shown in Fig (11). These data

are typical for angular settings in the range 0 to -60 arc-min. and also 0 to ± 150 arc-min..

IN-PLACE CALIBRATION EXPERIMENTS

The second stage of the evaluation was performed with the extensometer positioned on strain gaged specimens which in turn were installed in a tension-torsion test system. This allowed direct comparisons to be drawn between strain gage output and extensometer output as the specimens were subjected to biaxial loading within the material's elastic range. These experiments showed that torsional measurements made using both systems exhibited minimum hysteresis and were well behaved on passing through zero. As indicated in Fig. (12a), the hysteresis exhibited by the extensometer was about $6\mu\epsilon$ when the specimen was loaded over a torsional stress range of 32 mpa.

Crosstalk was further investigated by subjecting the specimen to axial loading and monitoring any resulting change in torsional strain output. These experiments confirmed the earlier results in that crosstalk was found to be small. It can be seen in Fig.(12b) that torsional strain output changed by about $\pm 6\mu\epsilon$ when the specimen was loaded axially over the range ± 120 mpa.

Finally, attention was directed at investigating the extensometer's performance at elevated temperatures. As already noted, a number of features had been incorporated into the design to ensure that the body of the device was at or near room temperature during elevated temperature tests. The effectiveness of these measures made it unlikely that the instrument's strain transfer characteristics at elevated temperatures would be significantly different from those at room temperature. Therefore, this stage of the evaluation was limited to investigating a number of electronic characteristics such as signal noise levels and signal stability.

After establishing base-line data at room temperature, signal noise levels were recorded under isothermal conditions at 232, 454, 538, and 650°C. It should be noted that specimen heating was by means of a 5kW radio frequency (RF) induction heater and that the heater incorporated a closed-loop temperature control system. This form of heating was found to cause drastic increases in signal noise levels. Thus, it was necessary to filter the signals from the extensometer to avoid problems with test system control. A variety of active and passive filtering systems were tried with mixed results. The best compromise was found to be obtained using passive filters with time constants of about 0.5 seconds. Typical strain signals recorded over 200 second time intervals after installing such filters are shown in Fig. (13). Behavior over this time interval was of particular interest as it approximates the time required for individual loading probes in multiaxial deformation experiments. Recordings of this type were also made over 24 hour periods to establish the influence of laboratory environment on signal stability.

EXPERIMENTS INVESTIGATING STRESS RELAXATION BEHAVIOR UNDER CYCLIC TORSIONAL LOADING

On completing the instrument development work, the scope of the in-place calibration experiments was expanded to investigate the feasibility of the generating stress relaxation data under torsional loading. By way of background, an attempt had been made to use stress relaxation data determined under uniaxial loading to quantify the kinematic state variable in the Robinson viscoplastic model (Refs. 10 and 11). However, interpretation of the data generated in these experiments was complicated by the extreme sensitivity of uniaxial strain measurements to thermal effects. In contrast, torsional strain measurements, as a result of being based on specimen rotations, are relatively unaffected by temperature changes and associated thermal expansion. For this reason, it was anticipated that less than ideal temperature control would not be a limiting factor in stress relaxation tests conducted under torsional loading.

TEST EQUIPMENT

Details of the test equipment are given in Table (1). In summary, the tests were performed on an MTS closed loop, electrohydraulic test system with provision for tension-torsion loading. The MTS system is controlled by a Digital Equipment Corporation PDP 8e computer and an Electronic Associates Inc. TR-10 Analog Computer. The type of specimen used is shown in Fig. (14). After fabrication, the specimen was solution annealed and postweld heat treated. Details of these heat treatments are given in Table (2) along with other information regarding the particular heat of material tested.

Prior to installation in the test system, the specimen was instrumented with four rectangular strain gage rosettes and seven chromel/alumel thermocouples. The strain gages were used to minimize bending during specimen installation and also to check out the performance of the biaxial extensometer at room temperature. Specimen heating was by means of a 5kW RF induction heater. The geometry of the heater load coil was designed to give a temperature profile within $\pm 5^{\circ}\text{C}$ of the nominal test temperature over a 25 mm gage length. The outputs from six of the chromel/alumel thermocouples were used to achieve this condition while the seventh was used for temperature control. The test setup described above is shown in Fig.15. Not shown in this figure is the water cooled heat shield which is positioned between the specimen and the biaxial extensometer during tests. This heat shield, in conjunction with those mounted on the sensors, prevents heating of the instrument by radiation.

PRELIMINARY EXPERIMENTS

At the start of this investigation, well established procedures were followed to ensure that the loading system and the various measurement systems were functioning properly. This preliminary work was aimed at ensuring the following:

1. The specimen was installed in the test system such that bending strains were within $\pm 5\%$ of the average strain.
2. The foil strain gage measurement system was functioning properly.
3. The biaxial extensometer was installed and functioning properly.
4. The temperature profile over a 25mm gage length was within $\pm 5^\circ\text{C}$ of the nominal test temperature.

The various procedures adopted to achieve these conditions are summarized in Table (3) along with the results obtained in the present experiment. As indicated in this table, the required conditions were met with one exception. This was that the best temperature profile that could be obtained was $538 \pm 20^\circ\text{C}$.

EXPERIMENTAL PROCEDURES

The experimental procedures used to investigate stress relaxation behavior under cyclic torsional loading were based in part on those used earlier in uniaxial experiments (Ref. 10). First, the specimen was cycled over a tensorial shear strain range of 0.56% using a ramp waveform and a nominal strain rate of $600 \mu\text{e}/\text{min}$. The required fully cyclically hardened condition was achieved after about ten cycles.

Stress relaxation experiments were then conducted from five starting locations on the stabilized hysteresis loops (Fig. 16). Details of the target values of stress and strain used for computer control are given in Table (4). Also shown in this table are the sequences of loading followed before and after individual stress relaxation experiments. The aim of these loadings was to return the material to the reference condition before starting the next experiment. Five stages of loading were required in stress relaxation tests conducted from the peak of the hysteresis loop while six stages of loading were required in tests conducted from other locations (Fig. 17).

TEST RESULTS

A typical stress-strain hysteresis loop for material in a fully cyclically hardened condition is shown in Fig. (18). Such loops were recorded directly using analog outputs from the test system's load cell and from the biaxial extensometer. One difficulty indicated in this figure is that strain rate was not controlled at the specified value, $600 \mu\text{e}/\text{min}$., with any degree of precision during the various stages of loading. Post-test analysis of the results showed that strain rates during elastic straining were as high as $900 \mu\text{e}/\text{min}$. while those during inelastic straining were as low as $300 \mu\text{e}/\text{min}$.

The results of the stress relaxation tests are shown in Fig. (19). One feature of the raw data is that a $\pm 1 \text{mpa}$ amplitude cycle is superimposed on the overall stress relaxation response. It was established that this cycling resulted from less than ideal control of torsional strain during the 0.167hr hold-periods. More specifically, the problem was caused by a deadband incorporated in the computer software to allow for noise on the signal being controlled. The cycling apparent in Fig. (19) clearly indicates that the size of the deadband selected, $\pm 5 \mu\text{e}$,

was too wide for precise stress relaxation testing. However, as the trends in the raw data were well defined, it was possible to construct average curves without much difficulty (Fig. 20). These curves subsequently were used to establish relationships between initial stress rate and starting stress on the hysteresis loop. The results of this analysis are shown in Fig. (21).

THEORETICAL CONSIDERATIONS: COMPARISON OF EXPERIMENT AND THEORY

As the results of the exploratory tests were reasonable consistent, it was possible to proceed to the final stage of the investigation. This involved use of the ORNL viscoplastic constitutive model to predict material response under conditions approximating those of the experiments. Because of the lack of multiaxial test data for 2-1/4 Cr-1Mo steel at elevated temperatures, the constants in this model were determined through uniaxial testing only. Thus, it was of considerable interest to determine how closely the model would predict behavior under other forms of loading, in this case simple shear.

THE VISCOPLASTIC CONSTITUTIVE EQUATIONS

An isothermal statement of the ORNL viscoplastic constitutive model is as follows:

$$\dot{\epsilon}_{ij} = \begin{cases} F^n \frac{\epsilon_{ij}}{\sqrt{J_2}} & ; \quad F > 0 \text{ and } S_{ij}\epsilon_{ij} > 0 \\ 0 & ; \quad \begin{matrix} F \leq 0 \\ \text{or} \\ F > 0 \text{ and } S_{ij}\epsilon_{ij} < 0 \end{matrix} \end{cases} \quad (1)$$

$$\dot{a}_{ij} = \begin{cases} \frac{H}{G^\beta} \dot{\epsilon}_{ij} - RG^{m-\beta} \frac{a_{ij}}{\sqrt{I_2}} & ; \quad G > G_0 \text{ and } S_{ij} a_{ij} > 0 \\ \frac{H}{G_0^\beta} \dot{\epsilon}_{ij} - RG_0^{m-\beta} \frac{a_{ij}}{\sqrt{I_2}} & ; \quad G \leq G_0 \text{ or } S_{ij} a_{ij} \leq 0 \end{cases} \quad (2)$$

in which,

$$\epsilon_{ij} = S_{ij} - a_{ij} \quad (3)$$

$$S_{ij} = \sigma_{ij} - \frac{1}{3} \sigma_{kk} S_{ij} \quad (4)$$

$$a_{ij} = \alpha_{ij} - \frac{1}{3} \alpha_{kk} S_{ij} \quad (5)$$

$$F = \frac{J_2}{K^2} - 1 \quad (6)$$

$$G = \frac{I_2}{K^2} \quad (7)$$

$$J_2 = \frac{1}{2} \epsilon_{ij} \epsilon_{ij} \quad (8)$$

$$I_2 = \frac{1}{2} a_{ij} a_{ij} \quad (9)$$

Here, ϵ_{ij} denotes the components of inelastic strain rate, K and α_{ij} are state variables and μ , n , m , β , R and H are material constants. Values of the constants for 2-1/4 Cr-1Mo steel at 538°C are as follows:

$$\mu = 3.6 \times 10^7$$

$$n = 4.0$$

$$\beta = 0.75$$

$$m = 3.87$$

$$R = 8.97 \times 10^{-8}$$

$$H = 9.92 \times 10^3$$

These values are consistent with the units of Ksi for stress, in/in for strain and time in hours. The scalar state variable, K, is taken to be constant for material in a fully cyclically hardened condition. The value of K used in the following analysis, 0.82, resulted from isothermal, uniaxial testing as did the other values listed above.

As indicated in equations (6) through (9), the stress dependence in this model enters through the second principal invariants of the applied stress and the internal stress. This infers that the material is initially isotropic and that it behaves independently of the third principal invariants. The validity of the latter assumption is examined later in the paper in light of the experimental results.

REDUCTION TO PURE SHEAR: COMPARISON OF PREDICTED AND EXPERIMENTAL RESULTS

In the case of simple shear, the equations (1) through (9) reduce to the following:

$$\dot{\epsilon}_{12} = \begin{cases} 1.39 \times 10^{-8} F^4 \operatorname{sgn}(\tau-s) & ; F > 0 \text{ and } \tau(\tau-s) > 0 \\ 0 & ; \begin{matrix} F < 0 \\ \text{or} \\ F > 0 \text{ and } \tau(\tau-s) < 0 \end{matrix} \end{cases} \quad (10)$$

$$\dot{s} = \begin{cases} \frac{7320}{|s|^{1.5}} \dot{\epsilon}_{12} - 3.17 \times 10^{-7} |s|^{6.23} \operatorname{sgn}(s) & ; s > s_0 \text{ and } \tau s > 0 \\ \frac{7320}{|s_0|^{1.5}} \dot{\epsilon}_{12} - 3.17 \times 10^{-7} |s_0|^{6.23} \operatorname{sgn}(s) & ; s \leq s_0 \text{ or } \tau s < 0 \end{cases} \quad (11)$$

in which
$$F = \frac{(\tau-s)^2}{0.67} - 1 \quad (12)$$

$$s_0 = \begin{cases} 0.01 \\ 0 \end{cases} \quad (13)$$

Here, $\dot{\epsilon}_{ij}$ is the tensorial component of inelastic shear strain rate, τ is the applied shear stress, and s is the shear component of the state variable α_{ij} .

The above equations were used to predict saturated stress-strain hysteresis loops under conditions approximating those of the experiments (Fig. 18). To avoid undue complication, the prediction shown in this figure was made assuming a single strain rate, $900\mu\epsilon/\text{min.}$, applied for the entire cycle. These equations were also used to predict stress relaxation behavior from various starting points on the hysteresis loops (Fig. 20). It should be noted that the model has no provision for predicting the "reversed" stress relaxation observed from points 3, 4, and 5. The horizontal lines constructed through these points are shown to emphasize the reversal of the experimental data.

DISCUSSION

In discussing the results of this investigation, consideration is given first to the performance of the biaxial extensometer. Of particular interest here are the characteristics important in high precision, probing type experiments. These include linearity, crosstalk, mechanical hysteresis, resolution and stability. This is followed by some general discussion on problems associated with traditional methods for investigating time dependent material behavior at elevated temperatures. Possible advantages resulting from the use of torsional loading are outlined and the results of some preliminary experiments are discussed in light of predictions made using the viscoplastic constitutive model. Finally, methods are discussed for quantifying the internal state variable and the constants in this model.

PERFORMANCE OF THE BIAxIAL EXTENSOMETER

One basic requirement for any strain measurement system is that its output should be linear over the full range of interest. As indicated in Fig. (7), the kinematic analysis performed during the preliminary design stage showed that this goal theoretically was attainable with the present design. This result subsequently was confirmed in bench calibration experiments conducted over angular ranges of ± 60 and ± 150 arc-min.. The data generated for the smaller range are shown for purpose of illustration in Fig. (10). The importance of this result is that the relationship between specimen strain and voltage output from the instrument is known with certainty even though conditions at the start of tests may not be well defined. This situation can arise, for example, as a result of less than ideal instrument installation or thermal expansion of the specimen. Provided the instrument's calibration is linear, voltages resulting from these effects can simply be nulled out prior to testing without compromising the accuracy of subsequent measurements.

Another important result shown in Fig. (10) is that the calibration data are repeatable for successive installations. This lent confidence to the assumption that calibrations performed on the bench would still apply when the instrument was installed on a specimen. Further confidence in this approach was obtained when strains measured using the biaxial extensometer were compared to those measured using foil strain gages. The results obtained using the two strain measurement systems were usually within 2% of each other.

As already noted, one problem peculiar to biaxial and multiaxial experiments is that interaction or crosstalk can occur between the various forms of loading and straining. This problem is particularly limiting in experiments involving small changes of inelastic strain or inelastic strain rate. The meaning of such experiments is lost if, for example, loading in the axial sense produces apparent torsional strains and vice versa. Also, crosstalk of this type clearly precludes any meaningful investigation of normality. This problem was approached in two ways during the design and development of the subject extensometer. First, crosstalk was recognized as being a problem from the outset and measures were taken to minimize its effect during the design stage. Second, in tests requiring extreme precision, techniques were developed to computer correct for crosstalk effects.

The effectiveness of the self-correcting feature designed into the instrument can be judged by the data shown in Fig. (11). Here, it can be seen that axial strains over the range $\pm 50,000 \mu\epsilon$ caused tensorial shear strain measurements to change by less than $30 \mu\epsilon$. A similar result is shown in Fig. (12b). In this case, loading a specimen over a ± 125 MPa axial stress range caused measurements of shear strain to change by less than $\pm 6 \mu\epsilon$. The linear relationship shown in this figure subsequently was used to computer correct for crosstalk effects in yield surface determinations conducted on 2-1/4 CR-1Mo steel at 20°C (Ref. 12). In these experiments, axial and torsional stresses and strains are sampled at 1 second intervals. Thus, for a known axial stress, the corresponding value of apparent torsional strain was computed using the expression $\Delta\epsilon_{12} = 0.05 \sigma_{11}$ and used to correct the measured value. A similar approach was used in these biaxial experiments to correct the measured values of axial strain. In this case, the analytical representation of crosstalk was $\Delta\epsilon_{11} = 0.29 \sigma_{12}$, where $\Delta\epsilon_{11}$ and σ_{12} have units of microstrain and MPa. Such corrections were found to be a prerequisite for the successful definition of small offset ($25 \mu\epsilon$) yield surfaces using the biaxial extensometer.

A further requirement in high-precision, probing type experiments is that the strain measurement system should not exhibit significant mechanical hysteresis. This is because differences in response between loading and unloading can provide a useful measure of change of material state. Clearly, any mechanical hysteresis in the instrumentation will complicate interpretations of this type. The need to minimize hysteresis influenced the design of the biaxial extensometer in two ways. First, flexural pivots were used in the lever-arms to act as bearings. These pivots, by utilizing sets of flat cross flexures, allow rotation between components without any associated rolling friction or backlash. Second, careful consideration was given to the method of mounting the instrument on specimens. The aim here was to avoid techniques which might lead to difficulties when the direction of loading is reversed or when loading passes through zero. The approach adopted was to use pairs of ceramic probes which grip the specimen by means of friction at three locations (Fig.2). The surfaces in contact with the specimen are flat resulting in line contact over 2.5mm lengths at each of the three locations. As indicated previously, preload springs are used to provide the frictional force necessary to prevent slippage.

The data shown in Fig. (12a) illustrate the effectiveness of these measures. These data were obtained by cycling a specimen over a 32 MPa

torsional stress range and recording the corresponding strain outputs from foil strain gages and the multiaxial extensometer. It was found that the extensometer exhibited only slightly more hysteresis than the strain gages the width of the hysteresis loop at zero load being about $6\mu\epsilon$. Also, the output from the extensometer was found to be well behaved when the direction of loading was reversed and when loading passed through zero.

High resolution is another important requirement for strain measurement systems supporting development of viscoplastic constitutive models. This characteristic plays a key role in experiments investigating behavior under multiaxial stress states. In these experiments, attempts are made to investigate inelastic response while maintaining the material in an unchanged state. This conflicting requirement can be approximated in probing type experiments in which very small changes in inelastic strain or inelastic strain rate are used as measures of inelastic response. Clearly, strain measurement systems used for this work must be capable of detecting these small changes which in practice requires near-microstrain resolution.

One feature of extensometers is that mechanical gain can be used to obtain high resolution. The kinematic analysis performed during the preliminary design stage showed that suitably designed lever-arm assemblies can provide significant mechanical magnification of specimen rotations. It was established that most magnification could be obtained by maximizing the length of lever BC and minimizing the length of lever CD (Fig. 3). Further gain was obtained by summing the rotations of the two lever-arm assemblies associated with a particular sensor. With the geometry used in the present experiments, one degree of specimen rotation produces a summed output of about 4 degrees at the attachment locations of the RVDTs. This meant that only modest amounts of electronic gain, $\times 100$, were needed to calibrate the instrumentation such that $\pm 3,000 \mu\epsilon \equiv \pm 10$ volts. Using this arrangement, the ability to detect voltage changes of the order of 3mV would theoretically give the required microstrain resolution.

In practice, however, the resolution of strain measurement systems are usually limited by electrical noise. This is particularly the case in elevated temperature tests where the heating system and the temperature control system can add to the problem. As previously noted, passive filters were used to minimize this difficulty. It can be seen in Fig.(13) that even after filtering, noise levels at 650°C are a factor of at least five greater than those at room temperature. Based on these results, it appeared that the aim of developing an instrument with near-microstrain resolution had been achieved in the case of tests conducted at room temperature. In the case of elevated temperature tests, the resolution was about $5 \mu\epsilon$.

Regarding signal stability, considerable effort was needed to achieve the results shown in Fig.(13). First, it was found necessary to control the laboratory air temperature to within $\pm 1^\circ\text{C}$. Further, in experiments requiring extreme precision, it was necessary to isolate the specimen, extensometer, and load frame from laboratory air currents. This was achieved by constructing an enclosure around the load frame and the ancillary equipment. Under these conditions, the strain signals from the extensometer exhibited negligible drift once thermal equilibrium had been established. It should be noted that the time periods investigated were relatively short, 24 hours and less. Such periods were consistent with early experiments which were short-term and exploratory in nature.

INVESTIGATION OF TIME DEPENDENT MATERIAL RESPONSE AT ELEVATED TEMPERATURES

Having developed instrumentation allowing precise biaxial strain measurement, the next problem addressed was how best to use this capability for investigating time dependent behavior at elevated temperatures. The two experimental approaches traditionally used for this purpose are the monotonic creep test and the stress relaxation test. Based on experience gained in previous uniaxial test programs, the preferred test method for the present experiments was the stress relaxation test and the preferred type of loading was pure torsion. Some background regarding these choices is given in the following.

One characteristic of creep data determined on test machines using dead weight loading is that the data usually exhibit considerable scatter (Ref. 13). Possible reasons for the variability include less than adequate control of conditions during initial loading and the test method's extreme sensitivity to errors in load and temperature. Also, difficulties arise as a result of the simple forms of extensometry used in the majority of these experiments. Poor dynamic response can result in unreliable strain measurements during the early stages of tests and less than adequate stability can result in errors in long term tests. Thus, although tests leading to steady state creep rates might appear advantageous from the modeling viewpoint, the associated experimental difficulties raise serious questions regarding the value of this test method in supporting constitutive equation development.

In contrast, the accuracy of stress relaxation data generated using closed-loop, electrohydraulic test systems appears less susceptible to experimental difficulties. Since these experiments are conducted under strain control, the magnitudes of both strain and strain rate are known with certainty during initial loading. Further, since total strain is simply held constant during the critical stage of the experiment, less demanding requirements are placed on the strain measurement system. One important advantage here is that the dynamic characteristics of load cell are limiting in detecting high inelastic strain rates rather than those of the extensometer. This is an advantage since load cells can detect dynamic events as rapid as 100in/in/sec. Also, since stress relaxation experiments are relatively short-term, unrealistic demands are not placed on the stability of the instrumentation. Another advantage of conducting these experiments on closed-loop, electrohydraulic test systems is that the material can be cycled over a known strain range between stress relaxation experiments and returned to a known reference condition. This approach allows a number of experiments to be conducted on a single specimen (Ref. 10).

Unfortunately, unless conducted with extreme care (Ref. 14), the stress relaxation test is not entirely free from experimental difficulties. One such difficulty is that the test method is extremely sensitive to temperature fluctuations when conducted under uniaxial loading. To illustrate, in tests conducted on 2-1/4CR-Mo steel at 538°C, a $\pm 5^\circ\text{C}$ or $\pm 1\%$ variation in specimen temperature causes stress to change by about $\pm 10\text{MPa}$. As can be seen in Fig. (19), stress variations of this magnitude will completely mask stress relaxation response in this material. It follows that both specimen temperature and laboratory temperature have to be controlled within very close limits if the production of misleading data is to be avoided.

A related difficulty arises in experiments in which radio frequency induction heaters are used to test ferritic steels. In these experiments, coupling can occur between specimen loading and specimen heating as a result of the magnetomechanical effect (Ref. 15). By way of explanation, the heat dissipated in inductively heated ferritic steels is a function of the material's ferromagnetic permeability. Also, it has been demonstrated that the permeability of these materials is a function of mechanical straining. Since specimen temperature typically is controlled by means of a single thermocouple located at a point on the specimen surface, straining an inductively heated specimen causes temperature to change at other locations in the specimen. The net result is that the temperature in the specimen gage length is not in a stabilized condition prior to conducting the stress relaxation test. As indicated above, the resulting temperature changes, occurring, say over a 25mm gage length, can invalidate the results of subsequent stress relaxation experiments.

One solution to these difficulties is to use an alternative form of loading. As noted earlier, torsional strain measurements are based on specimen rotations which theoretically are unaffected by temperature changes and associated thermal expansion of the specimen. This can be seen by inspection of the expression for torsional strain shown in Fig. (7). Also, the design of the biaxial extensometer is such that torsional measurements are insensitive to changes in laboratory temperature. This is because the symmetry of the instrument causes thermal effects to be self cancelling. In summary, therefore, it appeared that many of the difficulties experienced in previous uniaxial test programs would not be a factor in stress relaxation tests conducted under purely torsional loading. The exploratory tests described in the following were conducted to examine the feasibility of this approach.

The success of these experiments can be judged by the data shown in Figs. (18) through (21). Considering first the data shown in Fig. (18), no difficulty was experienced with the biaxial extensometer in cycling the specimen over a shear strain range of 0.56%. As in earlier experiments conducted at room temperature, no problems were experienced when the direction of loading was reversed or when loading passed through zero. Also, the extensometer exhibited no tendency to "walk" on the specimen with repeated cycling. The one difficulty which did occur during this stage of the experiment was that the nominal value of strain rate, 600 $\mu\epsilon$ /min., was not maintained constant within reasonable limits. This resulted from a problem with the computer control and was not related to the instrumentation being used.

The data shown in Figs. (19) and (20) demonstrated that the biaxial extensometer had sufficient stability and resolution to allow stress relaxation behavior to be investigated under purely torsional loading. Perhaps the most striking feature of the data shown in these figures is that the sense of the relaxation process reverses at a stress value of about 45 MPa. To illustrate, in the experiments conducted from starting stresses of 87 and 69 MPa, stress dropped by 21 and 9 MPa during the 600 second hold-periods. In contrast, stress increased during the hold-period in the other three experiments. For example, in the experiment conducted from a starting stress of 0 MPa, stress increased by about 7 MPa. This result confirms trends observed in earlier programs conducted on 2-1/4CR-Mo steel under uniaxial loading (Ref.10). As will be

discussed later, use will be made of this characteristic of the data to quantify the kinematic state variable in the viscoplastic constitutive model under consideration.

One apparent disadvantage of the experimental approach described above is that the magnitude of the stress changes occurring during the relaxation process are relatively small. If, however, consideration is given to the rate of change of stress, then the relaxation data shown in Figs. (19) and (20) can be shown to vary over several orders of magnitude. This is illustrated in Fig. (21) for the case of the initial stress relaxation rate. Whereas the stress changes occurring during relaxation fall within a ± 20 MPa range, the initial stress rates for the same data can be seen to cover a ± 1000 MPa/h range on average. It is reemphasized that these rates were measured using the test system's load cell. Bearing in mind the reliability of load cells, it was possible to place a high degree of confidence on the accuracy of these data.

Regarding the temperature insensitivity of the torsional strain measurements, no direct evidence has been presented thus far supporting this claim. Such evidence was obtained on completing the series of stress relaxation tests when the specimen was cooled from 538°C to room temperature. It was established that torsional strain output changed by less than $40\mu\epsilon$ during this process. In comparison, the thermal contraction associated with this cooling would have resulted in apparent axial strains of the order of $8000\mu\epsilon$. Based on these values, use of torsional loading reduced temperature sensitivity by at least two orders of magnitude.

In related activity, the magnetomechanical effect was shown not to be a factor in these experiments. In a series of exploratory tests conducted at 538°C, the specimen was loaded within its elastic range to a torsional stress of 45 MPa and held constant at this value for about 600 seconds. Both torsional stress and torsional strain were monitored during this period to investigate the stability of the signals. It was found that both signals remained constant within the limits of accuracy of the measurement system during the hold-period. Thus, if any thermal readjustments were occurring in the specimen as a result of the loading, the torsional strain measurement was totally unaffected by them. As stated earlier, this insensitivity to thermal effects is viewed as being an important advantage of torsional loading since it eliminates a major source of uncertainty.

COMPARISON OF PREDICTIONS WITH EXPERIMENTAL RESULTS AND DETERMINATION OF THE INTERNAL STATE VARIABLE

As noted earlier, it was of considerable interest to compare the data generated in the cyclic relaxation experiments to predictions made using the viscoplastic constitutive model. This was because this model was developed before the present results were available and also because the formulation of the model was based entirely on uniaxial test data. Thus, the results of the present experiments provided a totally independent check of the predictive capability of the model for a more fundamental form of loading, pure shear.

First, equations (10) through (13) were used to predict the stabilized hysteresis loop for conditions approximating those of the experiments. As indicated in Fig. (18), the theoretical and experimental results were found to be in reasonable agreement considering that the experimental values of temperature and strain rate varied from the nominal test values. Although falling short of a proof of the adequacy of the "J₂" assumption made in the theory, this comparison does provide some measure of its validity under the present conditions.

Equations (10) through (13) were also used to predict stress relaxation response from two of the starting locations on the stabilized hysteresis loop. These locations correspond to stress values of 87 MPa and 69 MPa. As indicated in Fig. (20), the predicted and the experimental data agree reasonably well. One feature of these data is that the viscoplastic model somewhat underpredicts the relaxation occurring in 600 seconds. It was not possible to make predictions of the curves from the other three starting locations as there is no provision in the model for predicting reversed stress relaxation.

One basic requirement for viscoplastic constitutive models incorporating internal state variables is that it should be possible to determine the current value of the state variable through simple phenomenological testing. The type of experiment described earlier, the stress-dip-test, can be used for this purpose. The particular value of starting stress, $\sigma_{12} = \tau^*$ at which the initial stress relaxation rate is zero can be obtained from equation (12) as follows:

$$F = \frac{(\tau^* - s)^2}{0.67} - 1 = 0 \quad (14)$$

giving in SI units

$$\tau^* - s = 5.6 \text{ MPa} \quad (15)$$

An experimental value of τ^* was determined from Fig. (21) to be 45 MPa. By substituting this value into equation (15) and solving for s , the value of the internal state variable was found to be 39.4 MPa. This value applies along the unloading side of the hysteresis loop, i.e., for the points 1 through 6 in Fig. (16), for material in a fully cyclically hardened condition at a temperature of 538°C.

It is of interest to note that the data generated in the stress-dip-test can also be used to determine the constants in the flow law. As indicated above, the internal state variable, s , is constant along the unloaded portion of the hysteresis loop. It follows that both σ_{12} and s are known at the start of each of the relaxation experiments. Further, the inelastic strain rates can be obtained for the start of the experiments using the expression,

$$\dot{\epsilon}_{12} = - \frac{\dot{\sigma}_{12}}{G} \quad (16)$$

where $\dot{\sigma}_{12}$ is measured directly and G is the shear modulus.

In the case where the material constants are unknown, the flow law is written,

$$\dot{\epsilon}_{12} = A \left[\frac{(\tau-s)^2}{0.67} - 1 \right]^n \quad (17)$$

The unknown constants, A and n, can be determined since τ , s and ϵ_{12} are known for a number of points. Optimized values of the constants can be determined by conducting a series of these experiments.

CONCLUSIONS

The following conclusions were drawn regarding the performance of the instrumentation, the practicality of the experimental approach proposed in this study, and the predictive capability of the Robinson viscoplastic constitutive model.

1. The ORNL biaxial extensometer gave excellent results when used to measure torsional strains at room and elevated temperatures. The instrument's output was linear over the strain range of interest, $\Delta\epsilon_{12} = 0.56\%$, and exhibited minimum crosstalk and hysteresis.
2. The torsional strain output of the biaxial extensometer was found to be insensitive to temperature changes in the specimen. This indicated that torsional loading can be used to advantage in generating stress relaxation data.
3. Theoretical predictions made using the Robinson viscoplastic constitutive model were in reasonable agreement with the experimental results obtained in this study.
4. The experiments conducted under torsional loading confirmed that kinematic state variables can be quantified by investigating stress relaxation behavior at various locations around stabilized stress-strain hysteresis loops.

REFERENCES

1. Robinson, D.N., Pugh, C.E., and Corum, J.M., "Constitutive Equations for Describing High-Temperature Inelastic Behavior of Structural Alloys," Proc. of Specialists Meeting on High-temperature Structural Design Technology of LMFBRs, IAEA Report IWGFR/11, pp. 44-57 (April 1976).
2. Liu, K.C., "Room Temperature Elastic-Plastic Response of Thin-Walled Tubes Subjected to Nonradial Combinations of Axial and Torsional Loadings," Pressure Vessels and Piping: Verification and Qualification of Inelastic Analysis Computer Programs, ASME Publication G00088, pp. 1-12, (1975).
3. Liu, K.C., and Greenstreet, W.L., "Experimental Studies to Examine Elastic-Plastic Behavior of Metal Alloys Used in Nuclear Structures," Constitutive Equations in Viscoplasticity: Computational and Engineering Aspects, ASME Publication AMD-Vol. 20, pp. 25-56 (December 1976).

4. Ellis, J.R., Robinson, D.N., and Pugh, C.E., "Behavior of Annealed Type 316 Stainless Steel Under Monotonic and Cyclic Biaxial Loading at Room Temperature," Nuclear Engineering and Design 47, pp. 115-123 (1978).
5. Ellis, J.R., Robinson, D.N., and Pugh, C.E., "Time Dependence in Biaxial Yield at Room Temperature," Journal of Engineering Materials and Technology, Vol. 105, pp. 250-256 (October 1983).
6. Robinson, D.N., "A Unified Creep-Plasticity Model for Structural Metals at High Temperature," ORNL/TM 5969, Nov. 1978.
7. Robinson, D.N., and Swindeman, R.W., "Unified Creep-Plasticity Constitutive Equations for 2-1/4 CR-1 Mo Steel at Elevated Temperature," ORNL/TM-8444, October 1982.
8. Slot, T., Stentz, R.H., and Berling, J.T., "Controlled-Strain Test Procedures," Manual on Low-Cycle Fatigue Testing, ASTM STP 465, American Society for Testing and Materials, pp. 100-128 (1969).
9. Troeger, H., "Considerations in the Application of Flexural Pivots," Automatic Control, Vol. 17, No. 4, pp. 41-46 (November 1962).
10. Swindeman, R.W., Robinson, D.N., "Experimental Methods to Determine the Kinematic State Variable in 2 1/4 CR-1 Mo Steel at High Temperature," ORNL-5776 (July 1981).
11. Swindeman, R.W., Williams, B.C., and Robinson, D.N., "Evaluation of the Mechanical Behavior of Vacuum Arc Remelted 2 1/4 CR-1 Mo Steel in Support of Constitutive Equation Development," Oak Ridge National Laboratory Report, ORNL/TM-8402 (December 1982).
12. Ellis, J.R., "Multiaxial Exploratory Testing," High-Temperature Structural Design Progress Report, Oak Ridge National Laboratory Report, ORNL-5930, pp. 7-23 (June 1982).
13. McAfee, W.J., and Sartory, W.K., "Materials Heat-to-Heat Variability Study: Part 1 - Compilation and Analysis of Data," Oak Ridge National Laboratory Report, ORNL-5604 (November 1980).
14. Hart, E.W., et al., "Phenomenological Theory: A Guide to Constitutive Relations and Fundamental Deformation Properties," Constitutive Equations in Plasticity, Edited by A.S. Argon, MIT Press (1975).
15. Jones, W.B., "Influence of the Magnetomechanical Effect in Testing Inductively Heated Ferritic Steel," Sandia Laboratories Report, Sand 82-0752 (May 1982).

Table (1) DETAILS OF TEST EQUIPMENT

| | |
|--------------------------|--|
| Loading System | MTS Tension-Torsion Test System with $\pm 200\text{kN}$ axial capacity and $\pm 2000\text{N} \cdot \text{m}$ torsional capacity. |
| Computer Control | Digital Equipment Corporation PDP 8e Computer in conjunction with an Electronics Associates Inc. TR-10 Analog Computer. |
| Software | ORNL enhanced version of FOCAL. |
| Specimen Type | Thin walled tubular design, the parallel section being 64mm long and the inside and outside diameters being 23.5mm and 26.04mm, respectively. |
| Specimen Heating | 5kW radio frequency induction heater with closed-loop temperature control. Details of the work coil are as follows: 84mm overall length; 48mm ID; 32mm spacing between the 4 turn windings; and manufactured from 5mm OD copper tubing. |
| Specimen Instrumentation | 4 foil rectangular strain gage rosettes in full bridge circuit for torsional measurement and half-bridge circuit for axial measurements. The two bridge circuits were set up using shunt calibration procedures so that $3000\mu\epsilon = 10 \text{ V}$. 7 intrinsic chromel/alumel thermocouples located over the 25mm gage length. |

Table (2) DETAILS OF THE MATERIAL TESTING

| | |
|--|--|
| <p>Materials Details</p> | <p>Vacuum arc remelted 2.25Cr-1Mo Steel, Cameron Iron Works Heat 56448, 50 mm-o.d. Bar Form</p> |
| <p>Heat Treatment Details</p> | <p>Solution anneal Heat to 927°C, hold for 60 min; cool at rate not exceeding 1°C/min. to 316°C; and air cool to room temperature. Postweld heat treatment Heat to 727°C, hold for 40 hr.; cool to 427°C at 1°C/min; and air cool to room temperature. Note: These heat treatments were performed under vacuum on finish-machined specimens.</p> |
| <p>Microstructural Characteristics</p> | <p>Equiaxed with grain size in the range 5-6 ASTM units Microhardness values in the range 110-125 (DPH) Microstructure consists of ferrite with globular $M_{23}C_6$ carbides and η carbide.</p> |

Table (3) RESULTS OF THE PRELIMINARY EXPERIMENTS

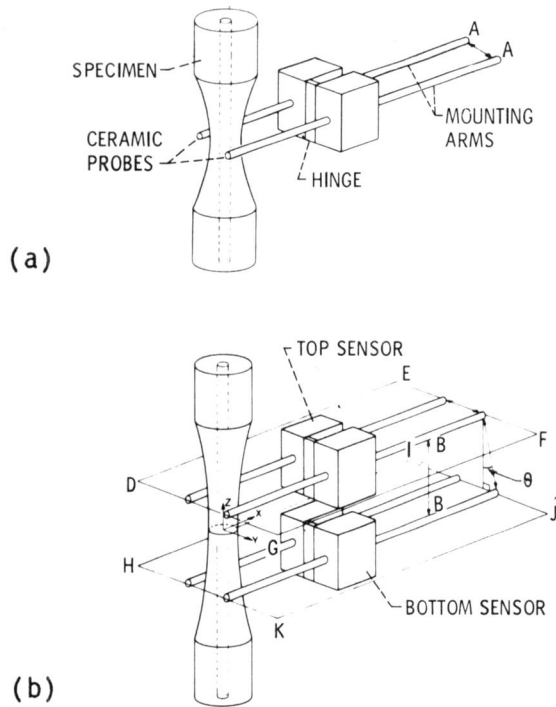
| Experimental Stage | Method Adopted | Results | |
|---|--|----------------------------------|----------------------------------|
| | | Target Value | Value Obtained |
| 1. Specimen Installation | Special purpose fixturing was used to get the specimen parallel and concentric with the acutator rod | 0.05 mm TIR ^a | 0.05 mm TIR |
| | Bending was minimized by successively shimming the load train, loading the specimen in compression, and measuring the resulting strain distribution. | within $\pm 5\%$ of average | $\pm 3\%$ of average |
| 2. Checkout of the strain gage measurement system. | Measurements of torsional stress and strain were made while the specimen was loaded within its elastic range. A value of shear modulus was then determined and compared to a hand-book value. ^b | $G=11.72 \times 10^6 \text{psi}$ | $G=11.67 \times 10^6 \text{psi}$ |
| 3. Checkout of the biaxialex-tensometer at room temperature | Measurements of torsional stress and torsional strain were made while the specimen was loaded within its elastic range. A value of shear modulus was then determined and compared to the value obtained using foil strain gages. | $G=11.67 \times 10^6 \text{psi}$ | $G=11.79 \times 10^6 \text{psi}$ |
| 4. Tuning the heating system | Adjustments were made to the load coil of the induction heater until the required profile was obtained over the 25mm gage length. The outputs from six chromel/alumel termocouples were used to achieve this condition. | $538 \pm 5^\circ\text{C}$ | $538 \pm 20^\circ\text{C}$ |

a. Total indicator reading

b. Nuclear Systems Material Handbook, Vol. (1)

TABLE (4) LOADING SEQUENCES USED TO INVESTIGATE STRESS RELAXATION
BEHAVIOR UNDER CYCLIC TORSIONAL LOADING

| EXPERIMENT NUMBER | LOADING SEQUENCE | LOADING TARGET | | HOLD-PERIOD (h) |
|-------------------|----------------------------|--|-----------------------------|--------------------------------|
| | | TENSORIAL SHEAR STRAIN ($\mu\epsilon$) | TORSIONAL STRESS (MP_a) | |
| 1 and 2 | 1 2 3 4 5 | 2800 -2800 2800 - 500 | 0 | 0 0 0.167 0 0 |
| 3 | 1 2 3 4 5 6 | 2800 -2800 2800 - 500 | 0 0 | 0 0 0 0.167 0 0 |
| 4 | 1 2 3 4 5 6 | 2800 -2800 2800 - 500 | 41.37 0 | 0 0 0 0.167 0 0 |
| 5 | 1 2 3 4 5 6 | 2800 -2800 2800 - 500 | 20.69 0 | 0 0 0 0.167 0 0 |
| 6 | 1 2 3 4 5 6 | 2800 -2800 2800 - 500 | 68.95 0 | 0 0 0 0.167 0 0 |



(a) Sensor positioned on specimen.
 (b) Use of two sensors for multi-axial measurements.
 Figure 1. - Basic approach.

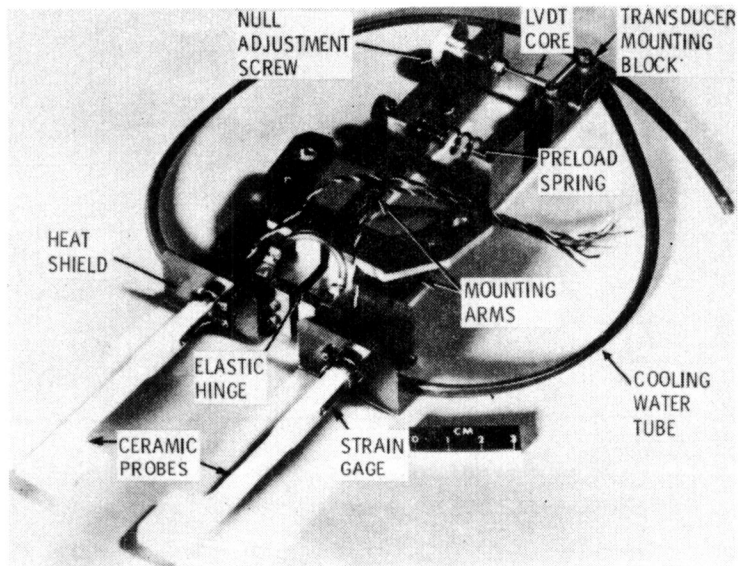


Figure 2. - Sensor assembly.

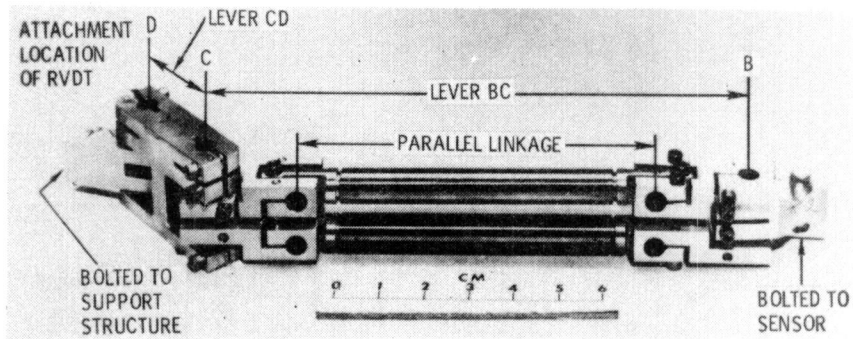


Figure 3. - Lever-arm assembly.

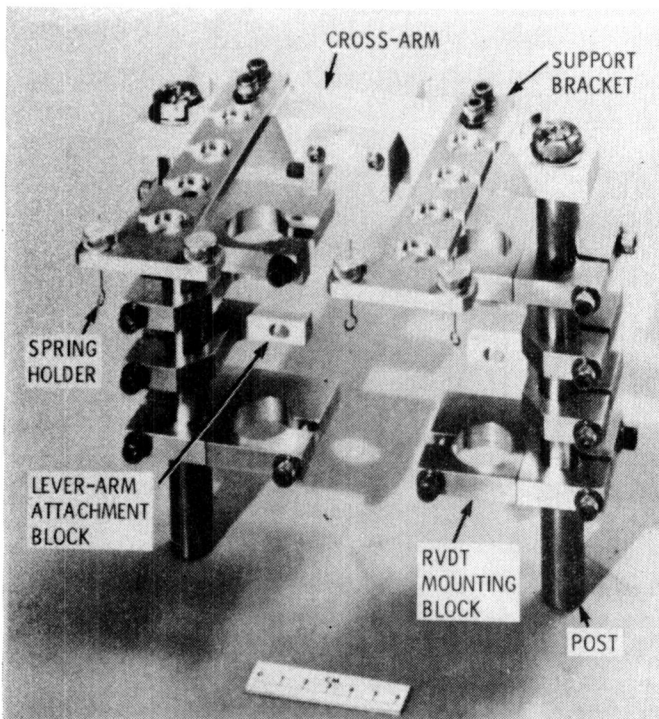


Figure 4. - Support structure.

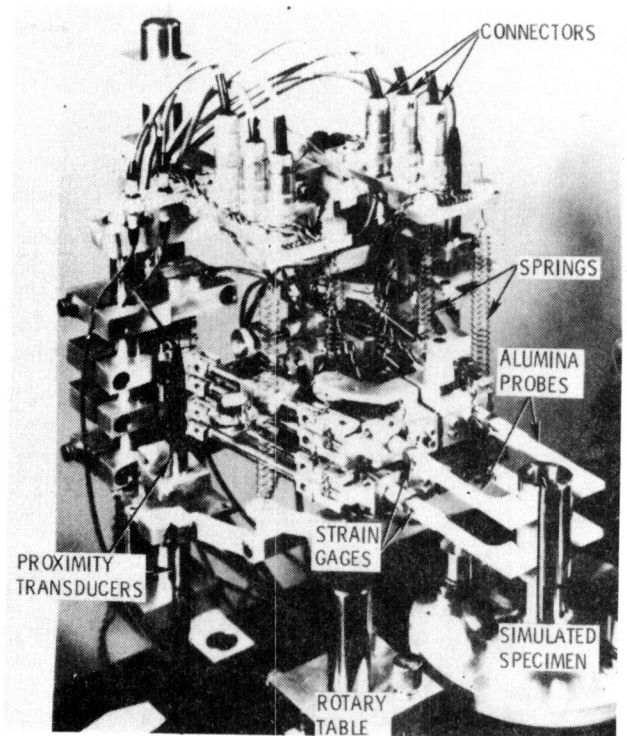


Figure 5. - Biaxial extensometer positioned on calibration fixture.

SIGN CONVENTION
 θ POSITIVE FOR COUNTERCLOCKWISE
 ROTATION ABOUT A
 α AND α' POSITIVE FOR CLOCKWISE
 ROTATIONS ABOUT D AND G

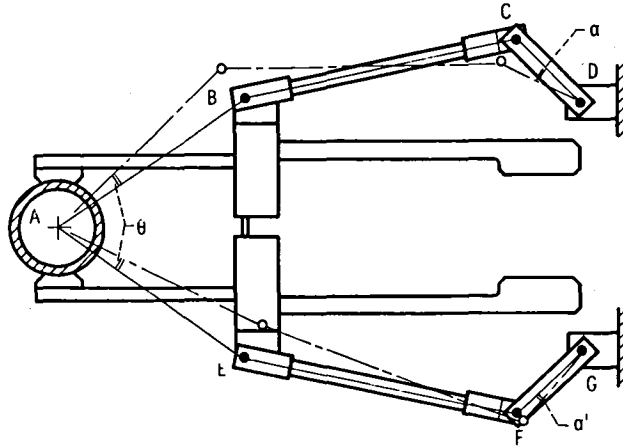


Figure 6. - Method of transmitting specimen rotation to fixed points on the support structure.

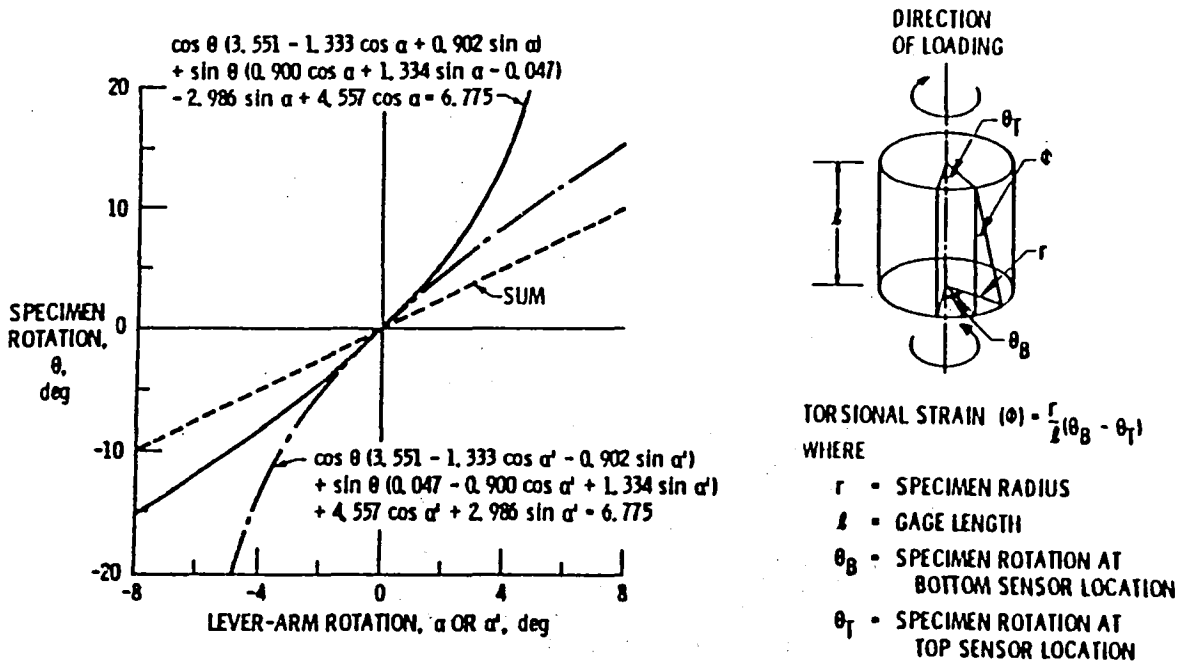


Figure 7. - Results of a kinematic analysis of the lever-arm assemblies.

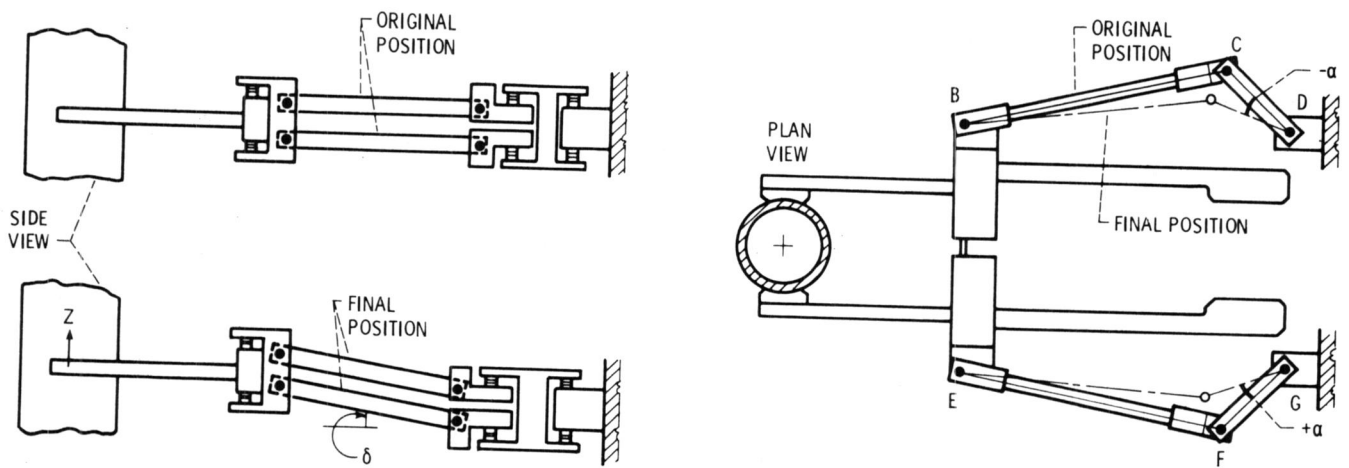


Figure 8. - Method of accommodating axial displacement.

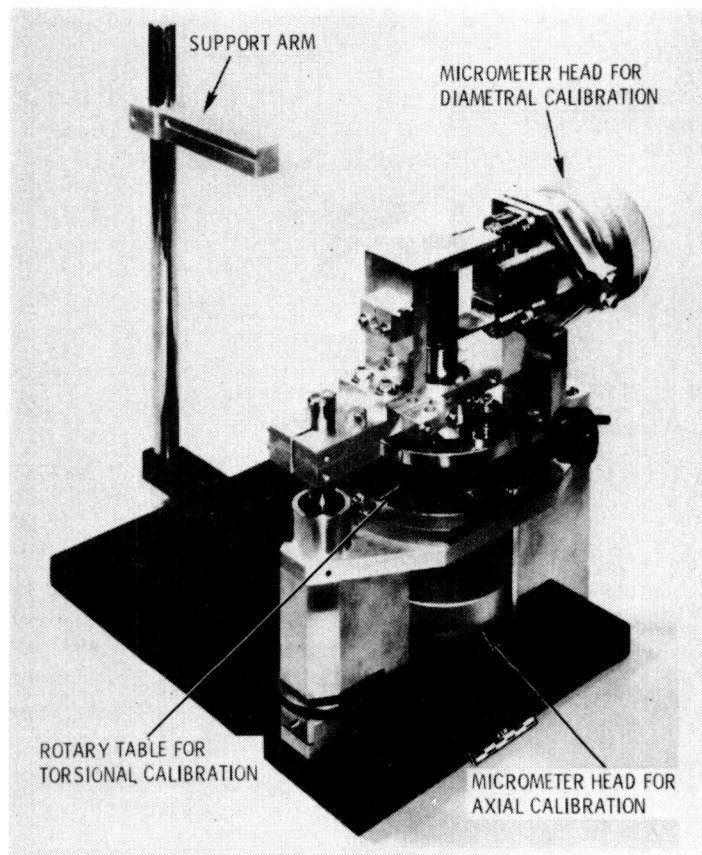


Figure 9. - Biaxial calibration fixture.

SCATTER BAND FOR EXPERIMENTS INVOLVING
REMOVAL AND REINSTALLATION OF THE EXTENSOMETER
SIX TIMES ON THE CALIBRATION FIXTURE

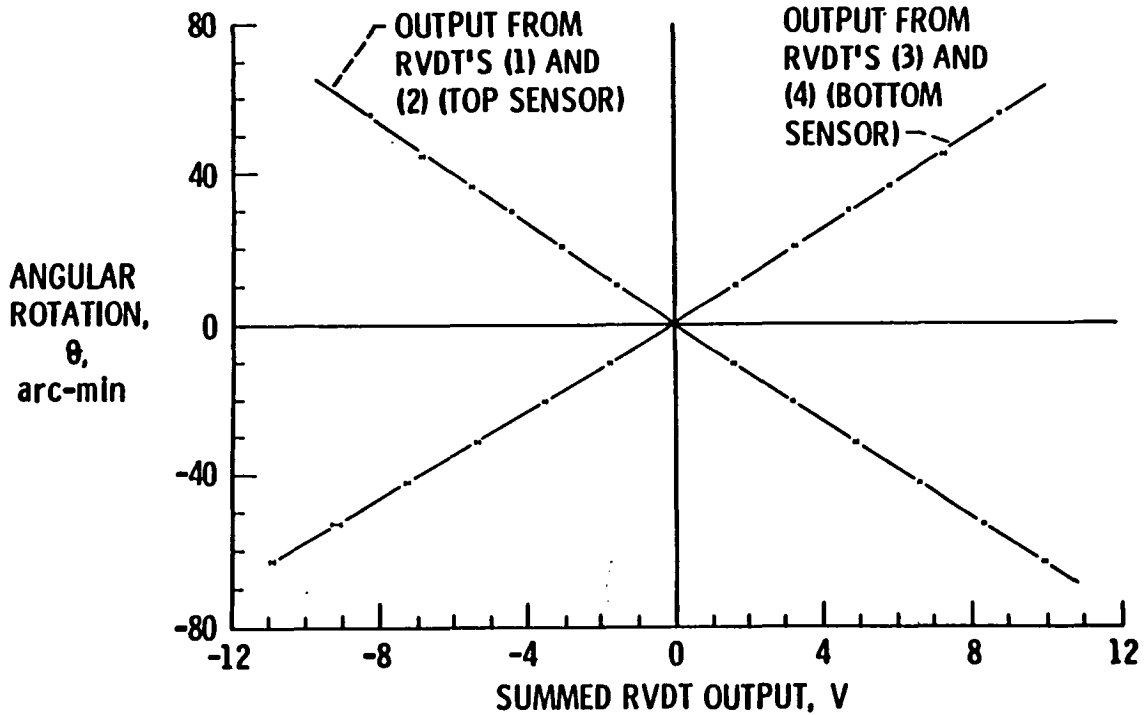


Figure 10. - Torsional calibration data for top and bottom sensors. (For a 25 mm-o.d. specimen and a 25 mm gage length, a relative rotation of ± 60 arc min between top and bottom sensors is equivalent to a tensorial shear strain of $\pm 4472 \mu\epsilon$.)

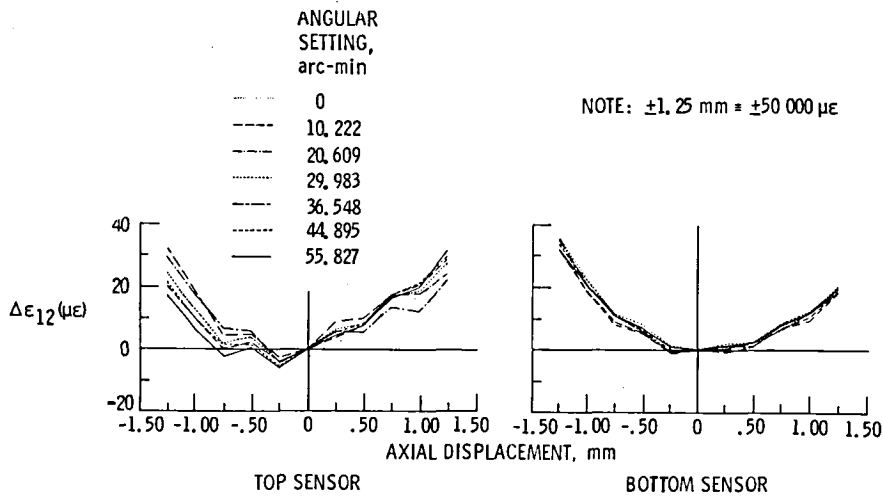
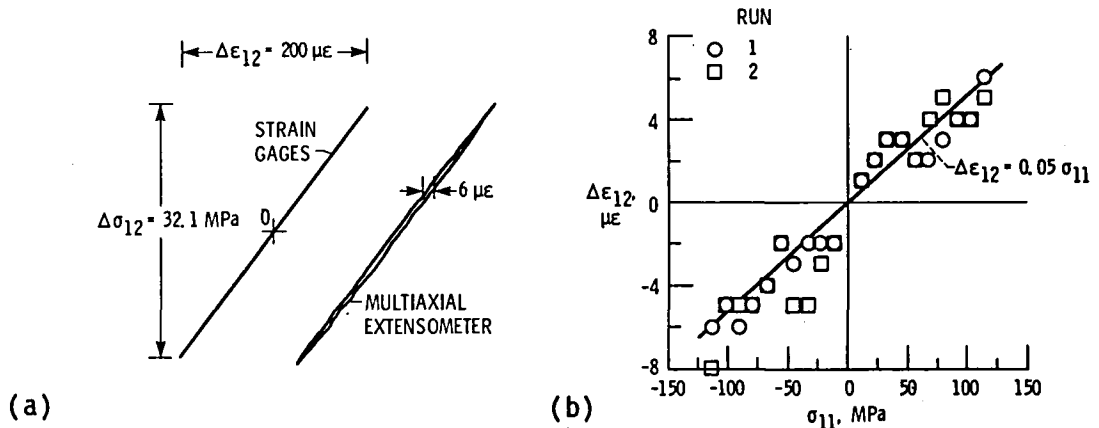


Figure 11. - Change in tensorial shear strain resulting from superimposition of axial displacement.



(a) Comparison of outputs from foil strain gages and the multi-axial extensometer.

(b) Effect of axial loading on torsional strain measurement.

Figure 12. - Results of in-place torsional calibration experiments performed at 20 °C. (The nominal calibration for all strain measurement systems was $3000 \mu\epsilon \equiv 10 \text{ V.}$)

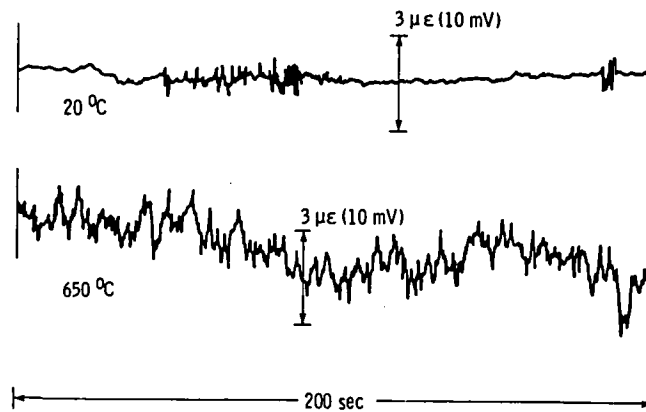
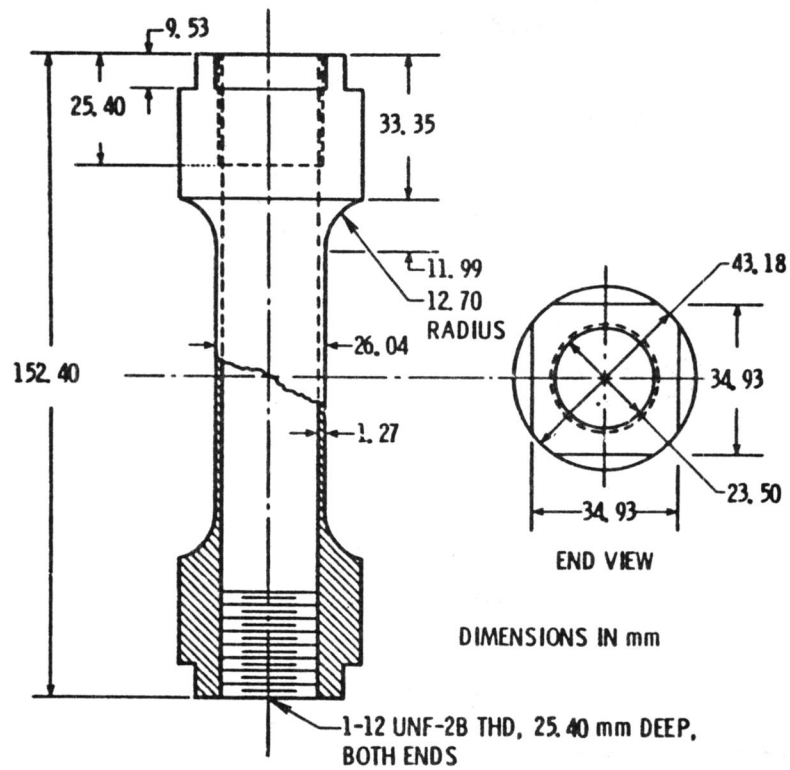


Figure 13. - Stability of torsional strain signals at 20 and 250 °C.

(A passive filtering system with a 0.5 second time constant was used in obtaining the signals shown.)



CS-84-2470

Figure 14. - ORNL tubular specimen design.

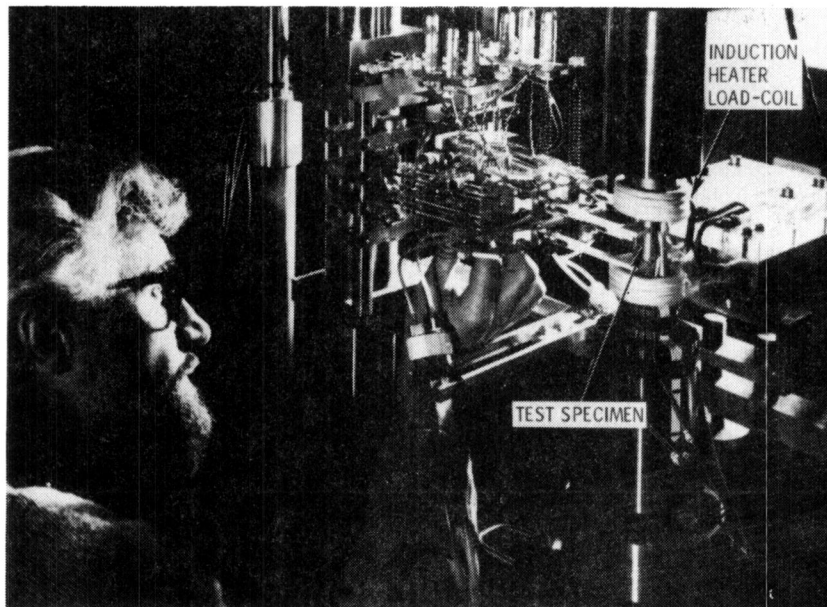


Figure 15. - Biaxial extensometer positioned on a tubular test specimen.

TEMPERATURE, 538° C; $\Delta\epsilon_{12} = 0.56\%$;
 $\dot{\epsilon}_{12} \approx 600 \mu\epsilon/\text{min}$

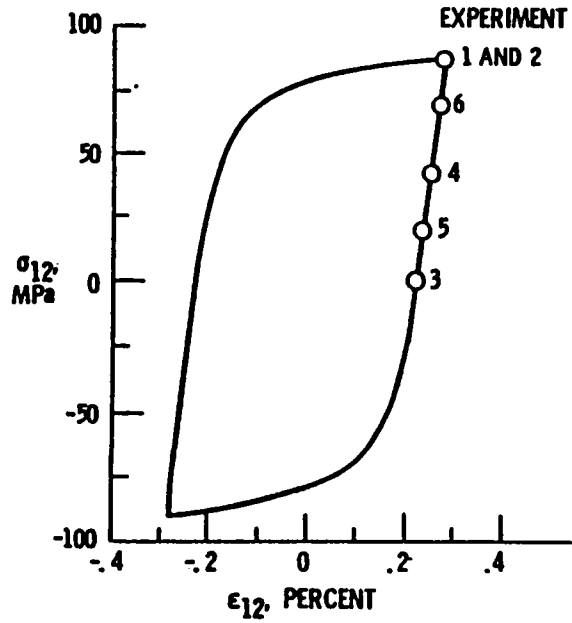


Figure 16. - Nominal stress-strain conditions at start of stress relaxation experiments.

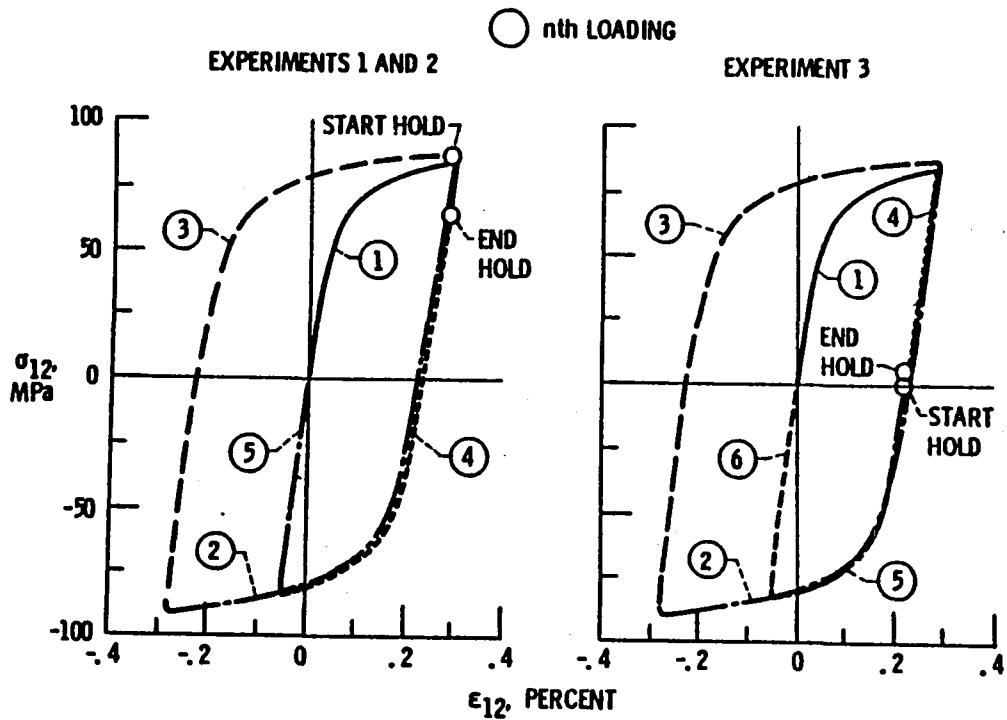


Figure 17. - Typical loading sequences.

TEMPERATURE, 538^o C; $\Delta\epsilon_{12} = 0.56\%$

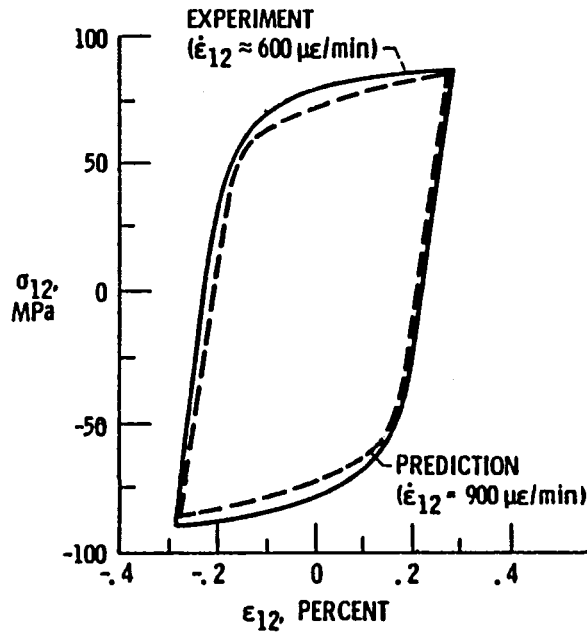


Figure 18. - Comparison of experimental and predicted stress-strain response.

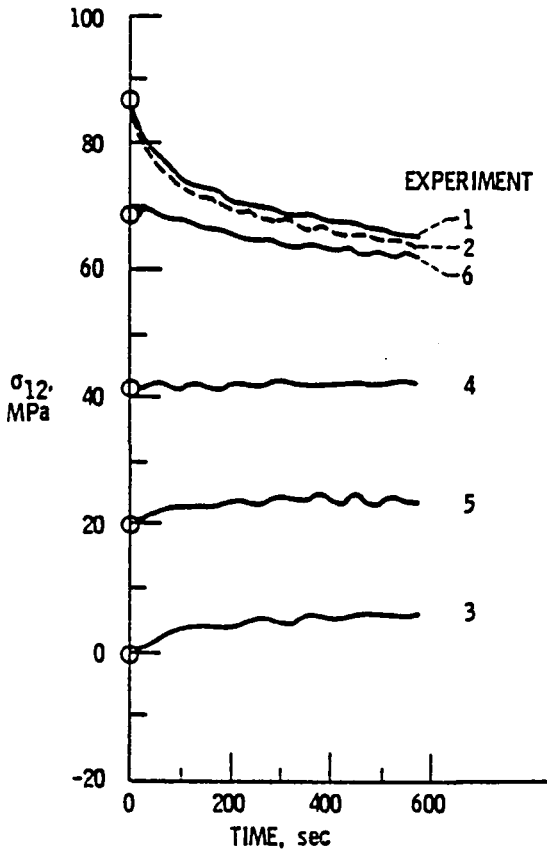


Figure 19. - Stress relaxation behavior from different starting stresses.

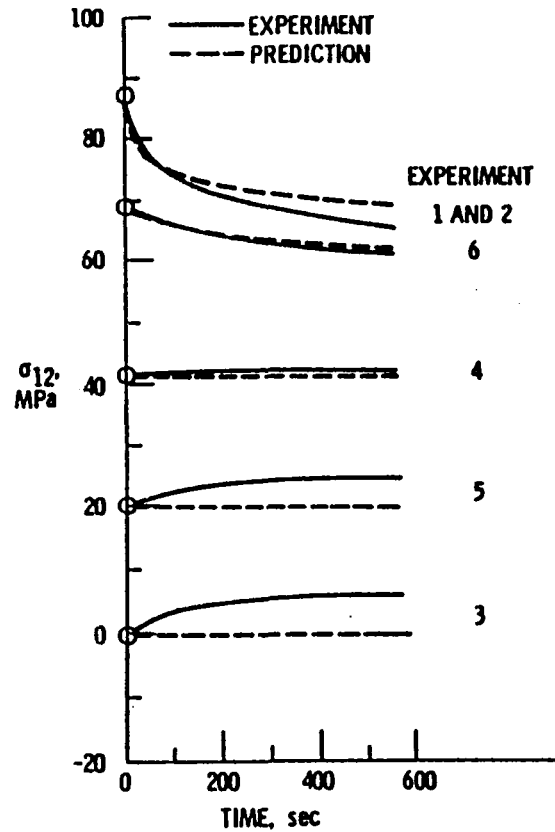


Figure 20. - Comparison of experimental and predicted stress relaxation behavior.

EXPERIMENTAL INTERCEPT, 45 MPa; PREDICTED INTERCEPT, 48 MPa

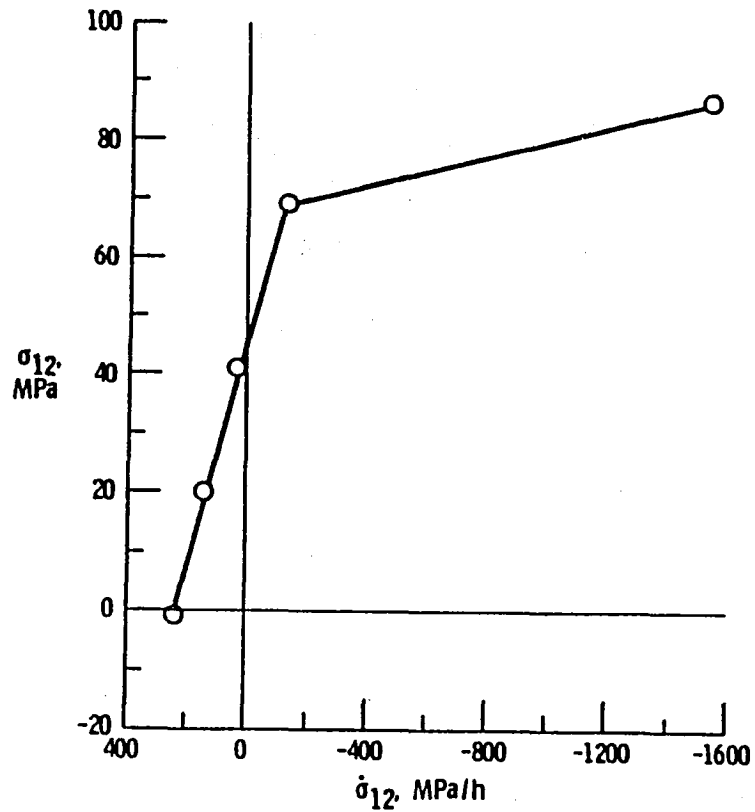


Figure 21. - Variation of initial stress relaxation rate with starting stress.